Lasers in Manufacturing Conference 2021

Effect of confined laser plasma plumes on the formation of LIPSS structures on stainless steel 316L

Anupam Ghosal[a,*], Olivier Allegre[a], Zhu Liu[a], Gordon Jones[b]

[a] *The University of Manchester, Manchester, M13 9PL, United Kingdom*
[b] *Waters Corporation, Wilmslow, Cheshire, SK9 4AK, United Kingdom*

Abstract

Laser-induced periodic surface structures (LIPSS) has been used for functionalisation of stainless steel surfaces. Hence, the control of the formation of the LIPSS structures is an essential aspect of laser surface texturing. In this work, picosecond pulsed laser irradiation (wavelength 355nm, pulse duration 10ps, frequency 404.7 kHz) was performed on stainless steel 316L under confined laser plasma plumes in atmospheric condition. The plasma plumes generated due to laser-metal interaction were confined by covering the metal surface with a transparent glass plate at varying distances (Δz = 0, 300, 450, 900 µm). The effect of the gap between metal and glass surface towards the formation of uniform LIPSS was studied experimentally. High spatial frequency LIPSS (HFSL) was produced by controlling the gap width. Low-spatial-frequency-LIPSS (LSFL) was observed at higher fluence along with scattered metal deposits on the surface. This work demonstrated the possibility of creating uniform HSFL using confined laser plasma plumes as the impacting medium.

Keywords: Laser-induced periodic surface structure (LIPSS); Nanostructure; Picosecond pulsed laser; Surface topography; laser plasma plume, high-spatial-frequency-LIPSS (HSFL)

1. Introduction

Periodic structures close to the wavelength of the laser generated on solids are known as laser induced periodic surface structures (LIPSS) and referred to as low spatial frequency LIPSS (LSFL) structures (Mannion et al., 2004). LIPSS structures with much smaller periods in the range of λ/4 – λ/8 are known as high spatial frequency LIPSS (HSFL) structures (Crawford & Haugen, 2007).

* Corresponding author. Tel.: +44-161-3064237.
E-mail address: anupam.ghosal@manchester.ac.uk

During the laser-material interaction, the intense laser pulse induces material removal and forms a high pressure and temperature laser plasma plumes containing the particles of the ablated material. The plasma plumes expand into the atmosphere and last for a very short interval. It has been used in the production of nanoparticles (Kolasinski et al., 2018). It is also used to assist in increasing the material removal and reducing the ablation threshold when laser processing underwater (Charee & Tangwarodomnukun, 2020). In this work, we present a method that confines the free expansion of the laser plasma plume using a glass cover and utilises it as one of the impacting parameters to affect the growth of surface structure on the surface of stainless steel 316L workpiece. The current work focuses on the generation of HSFL structures.

2. Materials and methods

2.1. The laser system

A picosecond laser was used to irradiate metallic surfaces to create LIPSS on their surface. The laser source is EdgeWave PX400-3-GH (EdgeWave GmbH Innovative Laser Solutions, Germany) and emitted linearly polarised light of wavelength 355nm with pulses of 10ps at a repetition rate of 404.7 kHz, as shown in figure 1. A scanning galvanometer (Digi-Cube Galvo) equipped with an F-theta lens having an effective focal length of 214.9 mm and a 3-axis positioning stage (Aerotech) was used to focus the laser on the surface of the workpiece. The laser beam was scanned as line scans using the galvanometer scan head under default atmospheric condition.

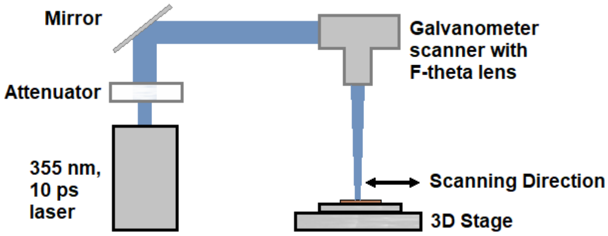

Fig. 1. Schematic of the picosecond laser system

2.2. Experimental method

The investigated material is mirror-polished AISI Stainless steel 316L (Goodfellow), with surface roughness Ra < 15 nm. The samples were cleaned in acetone and IPA ultrasonic baths, both before and after the process. A borosilicate glass cover (transmissivity ~90% at 355 nm) was placed over the surface of the workpiece, as shown in figure 2(a), to obstruct the laser plasma plume expansion. The fluence a value of 0.25±0.05 J/cm^2 at a frequency of 404.7 kHz was maintained throughout the study. The laser parameters of pulse-to-pulse distance (Δx), hatch distance (Δy) and the number of over-scans (Nsc) were varied in the range of 10 – 40 µm, 10 – 40 µm and 1 – 20 respectively, to identify cases of LIPSS structures. A representation of the laser parameters and scan direction is shown in figure 2(b). In the first step of the study, tests with variation in laser parameters were conducted on a workpiece without any glass cover, i.e. no obstruction on the expansion of the laser plasma plume. A test case was selected with well-defined LIPSS features from the first step, and a glass cover was placed on the surface of the workpiece for the purpose to investigate the impact of the laser plasma plume on the growth of LIPSS features, as shown in figure 2(a). The gap between the glass cover and the surface of the workpiece, i.e. Δz, was varied between 0 (glass cover directly over the workpiece surface) to 1 mm. The growth of high spatial LIPSS features was the primary objective of the study. The laser surface textures were topographically characterised scanning electron microscope (SEM) as well as atomic force microscopy (AFM) for imaging and profile measurements.

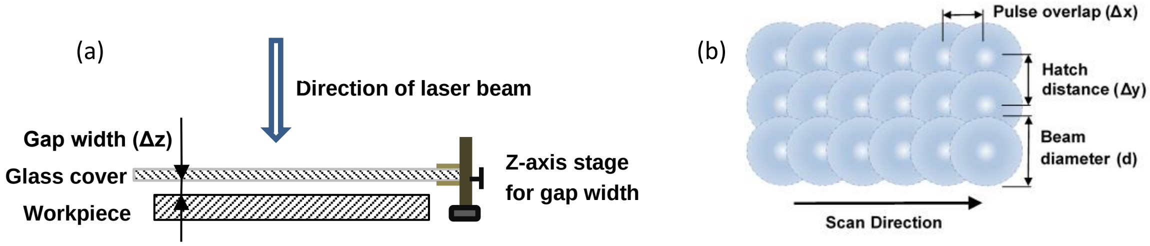

Fig. 2. (a) Schematic representation of the experimental setup; (b) Representation of the laser scan strategy

3. Results

3.1. Identification of LIPSS structures for no-glass cover condition

Single pulse ablation measurements for the fluence of 0.25±0.05 J/cm^2 show a spot diameter of 48 µm. The results obtained from modifying the laser parameters for the first step of the study show presence of visual ablation for pulse-to-pulse distance (Δx) and hatch distance (Δy) less than 15 µm. Focusing on the cases with presence of periodic structures, uniform low spatial frequency LIPSS features and sparse availability of high spatial frequency LIPSS features were observed for both Δx and Δy between 20 - 30 µm, i.e. 40 – 60% spot overlap at the number of over-scans (Nsc) between 14-19. The maximum accumulated fluence (Fa^{max}) was estimated using equations 1-3 (Mezera & Römer, 2019).

$$F_a^{max} = N_{sc}.F_0.\frac{\pi}{8(OL-1)^2}\left[1 + 2exp\left(\frac{-\pi^2}{8(OL-1)^2}\right)\right]^2 \qquad (1)$$

$$F_0 = \frac{8E_p}{\pi d^2} \qquad (2)$$

$$OL = 1 - \frac{\Delta x,y}{d} \qquad (3)$$

The result for pulse-to-pulse distance (Δx) = 23 µm and hatch distance (Δy) = 20 µm is shown in figure 3, with HSFL and LSFL features obtained at max. accumulated fluence 1.5 J/cm^2 and 6.8 J/cm$^{2.}$ respectively. The low spatial frequency LIPSS have a periodicity of 240±30 nm and a high peak-valley depth of 90±15 nm. The HSFL features present within the LSFL features show a periodicity of 65±5 nm. The presented case was selected for investigating the effect of confinement of the laser plasma plumes using glass cover over the surface of the workpiece.

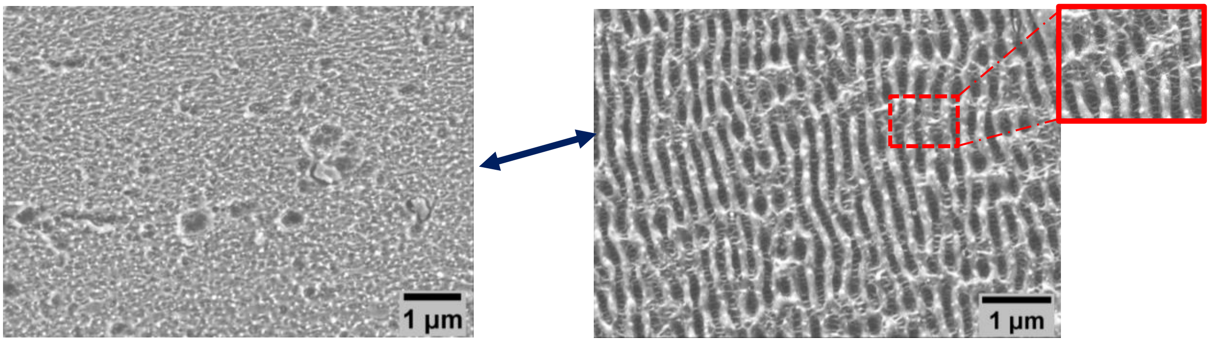

Fig. 3. HSFL (left) and LSFL (right) LIPSS features on no-glass cover case (Δx = 23 µm, Δy = 20 µm) obtained at max accumulated fluence 1.5 J/cm² and 6.8 J/cm² respectively. The polarisation vector of the laser is shown as a blue arrow.

3.2. High spatial LIPSS features growth under glass cover condition

After performing tests with the glass cover of the surface of the workpiece, a higher occurrence of HSFL features was noticed compared to the case with no glass cover. HSFL features were primarily observed in the max accumulated fluence between 1.2 J/cm² and 3.1 J/cm². Figure 4 presents the observed HSFL features with their estimated periodicities for the different gap width conditions. As observed, the periodicity of the features is higher at lower gap width condition, with an average periodicity of around 90 nm in the gap width region between 0 (no gap between the glass cover and workpiece surface) and 300 µm. AFM analysis was conducted on the surface demonstrated a roughness Ra = 11 nm and peak-to-valley depth as 35±10 nm. With the increase in gap width, the periodicity of the features is reduced, and the average periodicity is around 75 µm. However, the occurrence of HSFL features is also reduced. Figure 5 show the comparative HSFL features at the max accumulated fluence of 2.27 J/cm² at gap width 300 and 750 µm, having a periodicity of 90 nm and 75 nm, respectively. The presence of nano-bubbles can be observed on the HSFL feature at a gap width of 300 µm.

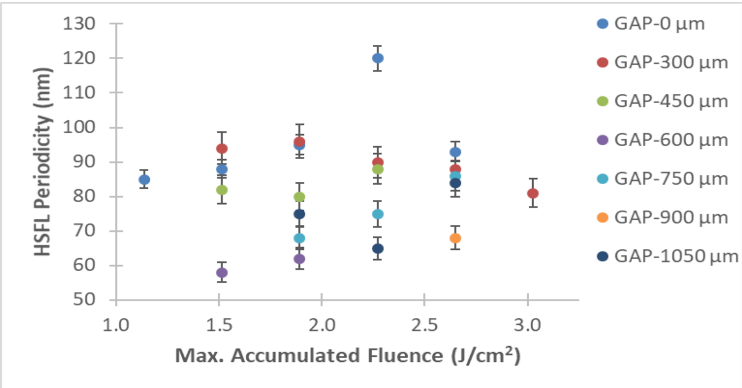

Fig. 4. HSFL features observed at max accumulated fluence for different gap width values.

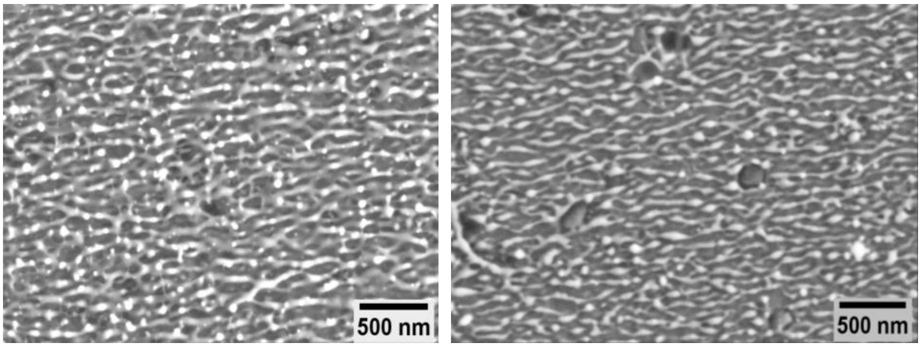

Fig. 5. HSFL features at a max accumulated fluence of 2.27 J/cm² at gap width 300 µm (left) and 750 µm (right)

Low spatial frequency LIPSS features were obtained at higher fluence region between 5.6 J/cm² and 6.8 J/cm². The periodicity of the features was 215±20 nm, and the width of the valleys is 75±15 nm. Similar to the no-glass cover case, bridge-like HSFL features were formed within the LSFL features show a periodicity of 60±10 nm. Also, the formation of melt pools was noted on the surface at smaller gap widths, and the frequency of the melt pools increased with the increase in the accumulated fluence. The formation of the melt pools was not seen in the normal case scenario, i.e. without the glass cover.

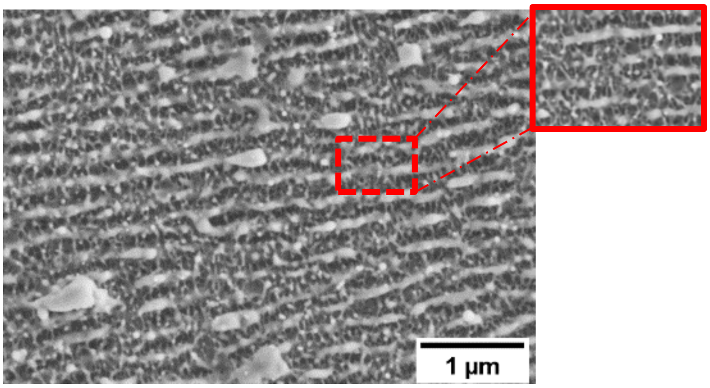

Fig. 6. LSFL features formed at an accumulated fluence of 6.8 J/cm² at gap width 300 µm, along with meltpools on the surface

4. Conclusion

In this work, we have shown experimentally that by blocking the free expansion of the laser plasma plumes with a glass cover over the surface of the workpiece, the growth of surface structures can be altered. High spatial frequency LIPSS structures growth was promoted on the surface for the same laser parameters compared to the normal case scenario of no-glass cover. Also, the periodic feature properties such as the periodicity and the peak-to-valley depth can be controlled to some extent.

High spatial frequency LIPSS structures are shallow structures compared to low spatial frequency LIPSS structures. Hence, HSFL features is useful in applications with the need of shallow laser features at nano-scale such as functionalization of the surface of electrode in mass spectrometer to improve the resistance to contamination.

Acknowledgements

The authors acknowledge the financial support received from Waters Corp. and the EPSRC CDT in Materials for Demanding Environments. The presented work is a part of ongoing research to improve the surface properties of electrodes in mass-spectrometers through laser surface texturing.

References

Charee, W., & Tangwarodomnukun, V. (2020). Laser ablation of silicon in water at different temperatures. *The International Journal of Advanced Manufacturing Technology*, *107*(5–6), 2333–2344. https://doi.org/10.1007/s00170-020-05182-4

Crawford, T. H. R., & Haugen, H. K. (2007). Sub-wavelength surface structures on silicon irradiated by femtosecond laser pulses at 1300 and 2100 nm wavelengths. *Applied Surface Science*, *253*(11), 4970–4977. https://doi.org/10.1016/j.apsusc.2006.11.004

Kolasinski, K. W., Gupta, M. C., & Zhigilei, L. V. (2018). Plume and Nanoparticle Formation During Laser Ablation. In *Encyclopedia of Interfacial Chemistry* (pp. 594–603). Elsevier. https://doi.org/10.1016/B978-0-12-409547-2.14045-4

Mannion, P. ., Magee, J., Coyne, E., O'Connor, G. ., & Glynn, T. . (2004). The effect of damage accumulation behaviour on ablation thresholds and damage morphology in ultrafast laser micro-machining of common metals in air. *Applied Surface Science*, *233*(1–4), 275–287. https://doi.org/10.1016/j.apsusc.2004.03.229

Mezera, M., & Römer, G. R. B. E. (2019). Model based optimization of process parameters to produce large homogeneous areas of laser-induced periodic surface structures. *Optics Express*, *27*(5), 6012. https://doi.org/10.1364/OE.27.006012